Appearance of three dimensionality in wall-bounded MHD flows

Klein, R. and Potherat, A.

Appearance of Three Dimensionality in Wall-Bounded MHD Flows

R. Klein and A. Pothérat

Applied Mathematics Research Centre, Coventry University, Priory Street, Coventry CV1 5FB, United Kingdom

(Received 3 August 2009; revised manuscript received 16 November 2009; published 21 January 2010)

We characterize experimentally how three dimensionality appears in wall-bounded magnetohydrodynamic flows. Our analysis of the breakdown of a square array of vortices in a cubic container singles out two mechanisms: first, a form of three dimensionality we call *weak* appears through differential rotation in individual 2D vortices. Second, *strong* three dimensionality characterized by vortex disruption leads on the one hand to a remarkable vortex array that is both steady *and* 3D, and, on the other hand, to scale-selective breakdown of two dimensionality in chaotic flows. Most importantly, these phenomena are entirely driven by inertia, so they are relevant to other flows with a tendency to two dimensionality, such as rotating, or stratified flows in geophysics and astrophysics.

DOI: 10.1103/PhysRevLett.104.034502 PACS numbers: 47.65.−d, 47.27.Cn, 47.32.cd

When a strong magnetic field is applied to an electrically conducting flow, the variations of all physical quantities are damped along it so the flow tends to two dimensionality. Broadly speaking, 2D magnetohydrodynamic (MHD) flows, like other 2D flows, tend to favor large, long-lived structures while fine, highly dissipative structures are the hallmark of 3D flows. Knowing the 2D or 3D nature of MHD and other flows is therefore key to understanding their behavior and global properties. This important question of fundamental physics also bears critical consequences in practical situations: in liquid metal heat exchangers or steel casting processes for instance, 3D turbulent flows are preferable to 2D flows to enhance heat and mass transport and favor homogeneous mixing. By contrast, in laboratory experiments, physicists use magnetic fields to artificially reproduce 2D flows [1]. Nevertheless, in all these problems, it is crucial but unclear, whether three dimensionality is present or not, and under which form. [2] clarified the "two dimensionalization" mechanism for a given MHD flow structure, of size $l_\perp$ and velocity U, by discovering that the Lorentz force diffused the momentum along a magnetic field $B\mathbf{e}_z$ over a length l_z, in a typical time $\tau_{2D}(l_\perp) = \tau_j(l_z/l_\perp)^2$ [σ and ρ are the fluid conductivity, density and $\tau_j = \rho/(\sigma B^2)$ is the Joule dissipation time that characterizes the Lorentz force]. The structure's inertia, on the other hand, increases with its turnover frequency $\tau_U(l_\perp)^{-1} = U/l_\perp$, and can induce three dimensionality when the latter becomes comparable to τ_{2D}^{-1}. Such inertia-induced 3D effects can occur in any 2D flow. [1,3] proved, for instance, that the meridional Ekman recirculations that drive a strong upward flow in tornadoes' eyes, acted alike in wall-bounded MHD flows. In tornadoes, indeed as in atmospheres, oceans and all rapidly rotating flows, the tendency to two dimensionality arises from the propagation of inertial waves along the rotation direction [4,5], so the same struggle between this tendency and inertia as in MHD flows determines the appearance of three dimensionality. Stratified flows too, where two dimensionality is driven along the density gradient, exhibit an analogous behavior [6]. Understanding how three dimensionality appears in MHD flows therefore bears some relevance to apparently remote problems such as weather forecast, predicting pollutant advection in the atmosphere, or describing some astrophysical flows. To this day though, although the mechanisms that favor two dimensionality are fairly well understood, most studies of the breakdown of two dimensionality have focused either on strictly 2D vortices, [7,8], or on single vortices or vortex pairs [9,10]. The mechanisms that ignite three dimensionality in more complex, wall-bounded flows, where boundary layers that develop along walls precludes strict two dimensionality, pose an open question. In this Letter, we propose an experimental answer to it: we prove that boundaries across the direction of two dimensionality allow inertia to sustain local differential rotation in nearly 2D structures. We also single out how the subtle interplay between inertia and the Lorentz force leads to stationary 3D flows that no model has foreseen, and to a scale-selective breakdown of two dimensionality in chaotic flows.

The principle of our experiment follows that of [1] in which a quasi 2D flow was produced by applying a constant homogeneous magnetic field across a square, shallow container made of electrically insulating walls and filled with liquid metal. The flow was termed "quasi 2D" to reflect its assumed invariance everywhere across the layer (i.e., along $B\mathbf{e}_z$), except in *Hartmann* boundary layers that develop along the walls orthogonal to the field, called *Hartmann walls*. Unlike this earlier experiment aimed at quasi 2D flows, our container is not shallow, but cubic with inner edge $L(= l_z) = 0.1$ m, so as to feature longer two-dimensionalization times τ_{2D} and thereby obtain 3D flows. The homogeneous field is directed along $\mathbf{e}_z$ too, so the two Hartmann walls are parallel to the ($\mathbf{e}_x$, $\mathbf{e}_y$) plane. The flow entrainment relies on the MHD equivalent of the tornado mechanism: in the same way these are triggered by a vertical flow due to ocean evaporation, columnar vortices of rotation axis $\mathbf{e}_z$ are driven in MHD flows by injecting electric current locally at one Hartmann wall only. 100 current injection electrodes are thus mounted flush at the bottom Hartmann wall only, with all or 16 of them, arranged in a 10×10 or 4×4 square lattice of step $L_i = 0.1L$ or $L_i = 0.3L$, alternately connected to either pole of a dc current generator. Hence, our base quasi 2D flow, obtained for low current and high magnetic field, is a square array of 100 or 16 cylindrical, quasi 2D vortices of axis $\mathbf{e}_z$, each of size $L_i \times L$, that rotate in alternate directions. Three dimensionality is monitored by measuring the electric potential ϕ at two sets of 121 points, covering two $(3\ \mathrm{cm})^2$ squares, respectively located on top and bottom Hartmann walls and aligned exactly opposite each other along $\mathbf{e}_z$ [10]. Since the electric potential is known not to vary across the very thin Hartmann layers, a quasi 2D flow would yield identical measurements on these two sets, while any difference between the two would betray 3D behavior. Furthermore, with the electric potential at a wall being proportional to the stream function just outside the Hartmann layer [11], our system provides a direct visualization of the flow patterns near either Hartmann walls. This allows us to visually identify quasi 2D structures. The flow is controlled by the injected current per electrode I (measured nondimensionally by a Reynolds number $\mathrm{Re}^0 = 2I/[\pi\nu(\sigma\rho\nu)^{1/2}]$) and by the externally imposed magnetic field intensity, measured by the *Hartmann number* $\mathrm{Ha} = LB[\sigma/(\rho\nu)]^{1/2}$. We track three dimensionality in established flows of increasingly high Re^0 in the interval $[0, 1.3 \times 10^5]$, for fixed values of Ha in [1092, 18220].

Regions of steady and unsteady flow regimes in the (Ha, Re^0) plane are reported on the stability diagram for $L_i = 0.1L$ on Fig. 1. A region of high magnetic field ($\mathrm{Ha} \gtrsim 7500$) and a region of low magnetic field ($\mathrm{Ha} < 7500$) clearly stand out. The physics of highest magnetic field regimes is essentially dominated by the very small values of τ_j, so that even our highest forcing produced a flow where all vortices had a turnover time $\tau_U(l_\perp) > \tau_{2D}(l_\perp)$. Corresponding flow patterns near the top and bottom Hartmann walls are identical at all times, which establishes their quasi two dimensionality [Figs. 1(a) and 1(b)]. In such flows, hardly any electric current remains in the bulk and the Lorentz force essentially acts on the flow by controlling the thickness of the Hartmann boundary layers $\delta_{\mathrm{Ha}} = L/\mathrm{Ha}$. These, in turn, exert a friction of characteristic time $\tau_H = \tau_j \mathrm{Ha}$ on all quasi 2D flow structures [2]. Since τ_H is Ha times longer than τ_j, the flow stability is determined by τ_H/τ_U. Indeed, it can be seen from Fig. 1 (top) that when the parameter $R_h = \mathrm{Re}^0/\mathrm{Ha} = \tau_H/\tau_U(L_i)$ exceeds the same critical value of $\mathrm{Re}^0_I/\mathrm{Ha} = 0.164$ for all $\mathrm{Ha} \geq 7500$, then 2D inertia destabilizes the array of alternately rotating vortices [Fig. 1(a)] into periodically oscillating quasi 2D vortex pairs [Fig. 1(b)]. For higher Re^0, the flow becomes chaotic, and even turbulent, but still remains

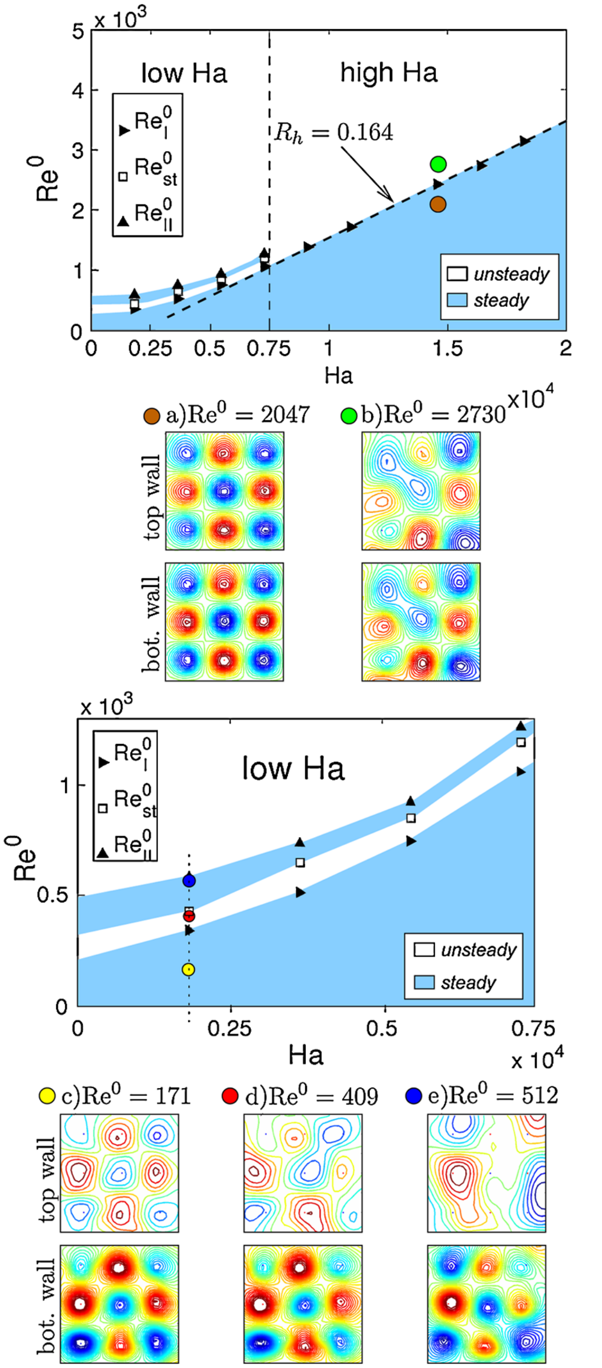

FIG. 1 (color online). Top: stability diagram giving critical Reynolds numbers $\mathrm{Re}^0_I(\mathrm{Ha})$, $\mathrm{Re}^0_{\mathrm{st}}(\mathrm{Ha})$ and $\mathrm{Re}^0_{II}(\mathrm{Ha})$ *vs.* Ha and snapshots of iso-ϕ lines, at the bottom and top Hartmann walls at $\mathrm{Re}^0 \lesssim \mathrm{Re}^0_I$ and $\mathrm{Re}^0 \gtrsim \mathrm{Re}^0_I$ for $\mathrm{Ha} = 1.458.10^4$, for which the flow is quasi 2D. Bottom: magnification of the top diagram in the low Ha region and snapshots of iso-ϕ lines, at the bottom and top walls at $\mathrm{Ha} = 1822$, for which the flow is 3D.

quasi 2D. This same instability and subsequent chaotic regimes were observed by [1] in a shallow container, but our results prove that the structures the author identified were indeed quasi 2D.

The above scenario changes significantly at lower fields ($\mathrm{Ha} < 7500$), for which $\tau_{2D}(L_i)$ is of the order of $\tau_U(L_i)$, even at low forcing. The first visible consequence is that although the steady base flow patterns near the bottom and top walls remain topologically identical, the flow is less intense near the top wall [Fig. 1(c)], implying that each columnar vortex in the array undergoes some differential rotation. We call *weak* this first manifestation of three dimensionality, as the structures it affects still extend from the bottom to the top wall without disruption of iso-ϕ surfaces. Iso-ϕ contours in different $(\mathbf{e}_x, \mathbf{e}_y)$ planes along $B\mathbf{e}_z$ are therefore homothetic. In fact, this phenomenon appears progressively when inspecting base flows from high to low values of Ha. In the intermediate range $3500 < \mathrm{Ha} < 7500$, periodically oscillating vortex pairs still appear at $\mathrm{Re}^0 = \mathrm{Re}^0_I(\mathrm{Ha})$, even though each of them is subject to differential rotation. A further novelty in this range of fields is that the flow stabilizes again when $\mathrm{Re}^0 = \mathrm{Re}^0_{\mathrm{st}}(\mathrm{Ha}) > \mathrm{Re}^0_I(\mathrm{Ha})$. This second steady regime is made of weakly 3D, steady vortex pairs. It destabilizes again as oscillating vortex pairing resumes much more erratically at $\mathrm{Re}^0 = \mathrm{Re}^0_{II}(\mathrm{Ha}) > \mathrm{Re}^0_{\mathrm{st}}(\mathrm{Ha})$.

Until now, weak MHD three dimensionality had only been predicted theoretically and numerically by [3,12], but not observed experimentally. These authors proved that 2D inertia-induced electric eddy currents between Hartmann layers and the bulk, that caused differential rotation and led columnar vortices to assume a 3D *barrel*-like shape. Weak three dimensionality is therefore a direct consequence of the presence of Hartmann walls.

Not unsurprisingly, three dimensionality manifests itself most spectacularly at the lowest magnetic field ($\mathrm{Ha} = 1822$), where τ_{2D} is highest. Compared to the intermediate field range, the pairing process at $\mathrm{Re}^0 \gtrsim \mathrm{Re}^0_I$ is only apparent on the top wall where the top end of vortices merge, while their bottom ends remain disjoint and nearly steady in the vicinity of the bottom wall [Fig. 1(d)]. This topological difference between flows near top and bottom Hartmann walls implies that vortices merge only partially across the container, as their reconnection does not take place everywhere along $\mathbf{e}_z$. We term this type of three dimensionality as *strong*, as opposed to the weak one, as it implies a disruption of iso-ϕ surfaces along $\mathbf{e}_z$ and the flows in different $(\mathbf{e}_x, \mathbf{e}_y)$ planes are not topologically equivalent anymore. Strong three dimensionality becomes even more blatant when the flow restabilizes at $\mathrm{Re}^0 = \mathrm{Re}^0_{\mathrm{st}}$. In this second steady regime, while the 10×10 array of vortices is still visible near the bottom wall, it connects in the bulk to a quite regular array of 5×5 alternately rotating vortices, visible near the top wall [Fig. 1(e)]. At $\mathrm{Re}^0 = \mathrm{Re}^0_{II}$, this flow destabilizes again through periodic oscillations that become chaotic at slightly supercritical forcing.

Unlike weak three dimensionality, strong three dimensionality appears through partial vortex pairing, a mechanism that is not *a priori* related to the presence of Hartmann walls. This second effect, and the even more spectacular fact that it can lead to steady 3D vortex arrays had not been predicted theoretically, so its dynamics now calls for theoretical analysis in MHD and other 2D flows.

We now turn our attention towards the last unsteady regime ($\mathrm{Re}^0 > \mathrm{Re}^0_{II}$ for $\mathrm{Ha} \leq 7500$ and $\mathrm{Re}^0 > \mathrm{Re}^0_I$ for $\mathrm{Ha} > 7500$), where we shall quantify the presence of weak and strong three dimensionality. Since flow visualizations are not as revealing in these regimes, we shall instead analyze the correlations of the fluctuations of electric potential gradients $\partial_y \phi'$ around their time average, between pairs of measurement points aligned opposite each other on bottom and top Hartmann walls (denoted by subscripts b and t, respectively). Weak and strong three dimensionality are identified by comparing two types of correlations

$$C'_1 = \frac{\sum_{t=0}^{T} \partial_y \phi'_b(t) \partial_y \phi'_t(t)}{\sqrt{\sum_{t=0}^{T} \partial_y \phi'^2_b(t) \sum_{t=0}^{T} \partial_y \phi'^2_t(t)}},$$

$$C'_2 = \frac{\sum_{t=0}^{T} \partial_y \phi'_b(t) \partial_y \phi'_t(t)}{\sum_{t=0}^{T} \partial_y \phi'^2_b(t)},$$

where T is the duration of our recorded signals. Values of C'_1 below unity reflect strong three dimensionality only, while C'_2 differs from unity whenever either weak or strong three dimensionality is present. To assess the link between inertia and three dimensionality, we have plotted the variations of spatial averages $\langle C'_1 \rangle$ and $\langle C'_2 \rangle$ against the *true* interaction parameter $N_t = \tau_{u'}/\tau_{2D}(L_i)$ [13], that measures the relative influence of Lorentz to inertial forces in vortices at the injection scale ($\tau_{u'} = L_i/U_{\mathrm{RMS}}$ is a turnover time built on a typical RMS of velocity fluctuations $U_{\mathrm{RMS}} = \langle \langle \partial_y \phi'_b \rangle_t^{\mathrm{RMS}} \rangle / B$, as in [10]). First, the fact that all our measurement points collapse into two single curves $\langle C'_1 \rangle(N_t)$ and $\langle C'_2 \rangle(N_t)$ proves that the three dimensionality we detect is exclusively of inertial nature. Second, since $\langle C'_2 \rangle(N_t) < \langle C'_1 \rangle(N_t)$ for all N_t, weak three dimensionality is always present, albeit in minute amounts at high B. This supports [3]'s theoretical prediction that the *barrel* effect exists whenever inertia is present in the flow, and vanishes at high N_t. Also, the increase of correlations with N_t is in line with [14] who found analytically that in the absence of inertia, the correlation length along the field increased with B.

More light is shed on the precise variations of $\langle C'_1 \rangle(N_t)$ and $\langle C'_2 \rangle(N_t)$ by inspecting the power spectral density from signals acquired at points aligned opposite each other on either Hartmann walls, and corresponding snapshots of the flow patterns on Figs. 2(a)–2(d). In the high N_t regime where $\langle C'_2 \rangle < \langle C'_1 \rangle \lesssim 1$, both spectra overlap over the whole frequency spectrum: the dynamics of vortices of all sizes is therefore 2D to a very good approximation. [Fig. 2(d)].

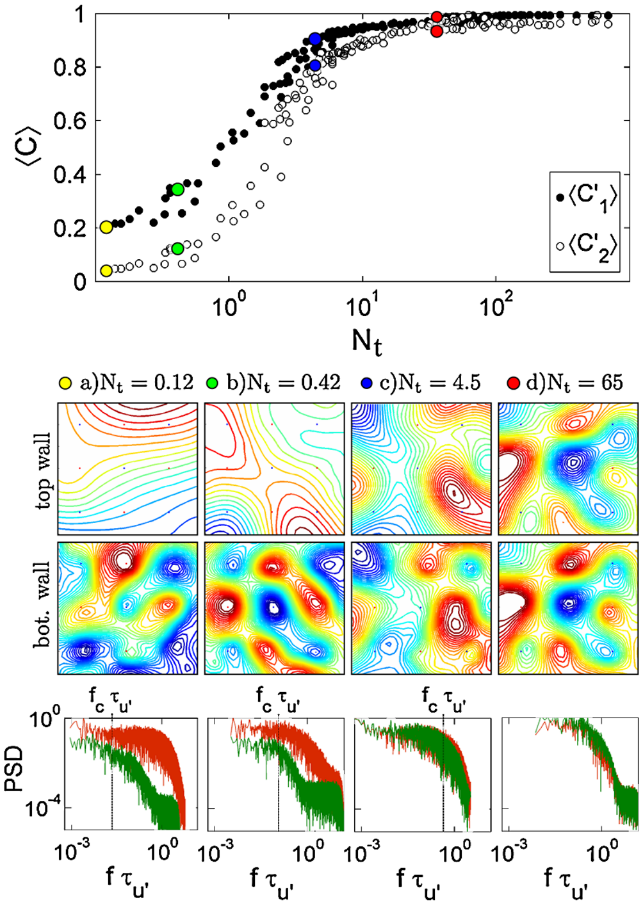

FIG. 2 (color online). Top: Spatially averaged correlations $\langle C_1' \rangle$ and $\langle C_2' \rangle$ *vs.* true interaction parameter N_t. Bottom: snapshots of iso-ϕ lines, (a)–(d) and corresponding power spectral density of $\partial_y \phi(x, y, t)$ at bottom (red) and top walls (green).

The sharp drop of both correlations at intermediate N_t is initiated by a loss of energy in the smaller scales near the top wall [Fig. 2(c)]. Structures of the corresponding size are generated near the bottom wall but because of their large aspect ratio $L/l_\perp$, the Lorentz force takes a longer time $\tau_{2D}(l_\perp)$ to diffuse their momentum up to the top wall, than it does for larger structures. When this time exceeds their turnover time $\tau_U(l_\perp)$, inertial effects disrupt them before they can reach the top wall, so they become 3D. Larger vortices, on the other hand, have a smaller aspect ratio, a shorter $\tau_{2D}(l_\perp)$, so they remain essentially quasi 2D. A cutoff scale, identified by a frequency $f_c(N_t)$ in the spectra, separates vortices that are "wide" enough to be quasi 2D from the smaller, 3D ones. When N_t decreases, $f_c(N_t)$ decreases as three dimensionality contaminates larger and larger scales [Fig. 2(b)], until even the largest structures become 3D and hardly any flow remains near the top wall [Fig. 2(a)].

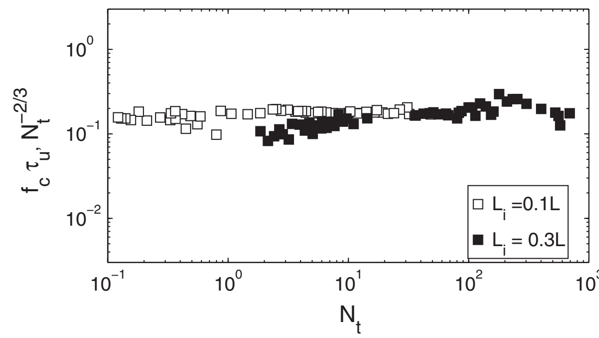

FIG. 3. Cutoff frequency f_c, normalized by the large scale eddy turnover frequency $\tau_{u'}^{-1}$, vs N_t.

We have calculated f_c precisely, by seeking the maximum of the function $g(f_p) = \langle C_1'(f_p) \rangle$, obtained by applying a low-pass filter of variable cutoff frequency f_p to $\partial_y \phi_b'(t)$ when calculating C_1'. Figure 3 shows that for both $L_i = 0.1L$ and $L_i = 0.3L$, f_c satisfies $f_c \simeq 1.7\tau_{u'}^{-1} N_t^{0.67}$ to a great precision, over the whole range of control parameters Ha and Re^0. This general law gives a clear estimate for the minimum frequency of vortices that are affected by 3D inertial effects, in the spirit of the heuristic law $k_{3D} \backsim N_t^{1/3}$ given by [2] for the minimum transverse wavelength of 3D vortices. Furthermore, since this scale-selective breakdown process depends on $\tau_{u'}$ and τ_{2D} only, a similar law should hold in other flows with a tendency to two dimensionality, albeit with a different expression of τ_{2D}.

We are grateful to the Electroheat group from Ilmenau University for lending us their Magnet and to the Deutsche Forschungsgemeinschaft for funding this work (Grant No. PO1210/4-1).

[1] J. Sommeria, J. Fluid Mech. **170**, 139 (1986).
[2] J. Sommeria and R. Moreau, J. Fluid Mech. **118**, 507 (1982).
[3] A. Pothérat *et al.*, J. Fluid Mech. **424**, 75 (2000).
[4] H. P. Greenspan (Cambridge University Press, Cambridge, England, 1969).
[5] R. Akkermans *et al.*, Phys. Fluids **20**, 116601 (2008).
[6] J. Paret *et al.*, Phys. Fluids **9**, 3102 (1997).
[7] O. Zikanov and A. Thess, J. Fluid Mech. **358**, 299 (1998).
[8] A. Thess and O. Zikanov, J. Fluid Mech. **579**, 383 (2007).
[9] D. Sous *et al.*, Phys. Fluids A **16**, 2886 (2004).
[10] R. Klein, A. Pothérat, and A. Alferenok, Phys. Rev. E **79**, 016304 (2009).
[11] A. Kljukin and A. Thess, Exp. Fluids **25**, 298 (1998).
[12] B. Mück *et al.*, J. Fluid Mech. **418**, 265 (2000).
[13] B. Sreenivasan and T. Alboussière, J. Fluid Mech. **464**, 287 (2002).
[14] G. Rüdiger, Astron. Nachr. **295**, 275 (1974).